

Contents lists available at ScienceDirect

Remote Sensing Applications: Society and Environment

journal homepage: www.elsevier.com/locate/rsase



Traditional agroecosystems for urban temperature regulation: a remote sensing analysis of an historical palm grove

Ignacio Melendez-Pastor

Department of Agrochemistry and Environment. Miguel Hernández University of Elche (Spain), Av/ Universidad s/n. Edificio Alcudia, Elche, Alicante, 03202, Spain

ARTICLE INFO

Keywords: Urban heat island Agroecosystems Palm grove Urban greening Semiarid

ABSTRACT

The current expansion of urban areas means that an ever-increasing population is affected by urban heat islands (UHI). Different strategies have been developed to mitigate the effects of UHI, such as the implementation of new urban green areas. However, before the expansion of green areas, it was common to see agroecosystems that have been systematically transformed into builtup areas. Fortunately, there are still traditional agroecosystems, such as the World Heritage Palm Grove (WHPG) of Elche (Spain), whose effect on urban temperature regulation requires evaluation. A time series of satellite remote sensing images was used to analyse the dynamics of land surface temperature (LST). Different statistical procedures (e.g., Kruskall-Wallis test, Friedman test) were used to determine the temperature attenuation effect throughout the year by the diverse land covers and green areas. Significant differences in LST between the agroecosystem conserved within the WHPG and the rest of the city were observed, with their cooling effect extending several hectometers around its perimeter. It was shown that the date palm grove and its traditional irrigation system have a significant regulatory effect on the LST and, consequently, on the attenuation of heat islands. This study highlights the need to conserve or regenerate traditional agroecosystems within cities, since in addition to being adapted for centuries to existing environmental conditions, they provide numerous ecosystem services and improve natural temperature regulation in urban environments. The traditional agroecosystem of the Elche Palm Grove has a significant thermal regulation capacity and is highly adapted to the limited water resources typical of semi-arid areas.

1. Introduction

Urban population growth is a global phenomenon and is expected to continue in the coming decades (UN DESA, 2019). This process of increasing urban population is accompanied by a global expansion of urban areas and associated land covers (Liu et al., 2018). Cities in an early period of social development and urbanization are typically characterized by densification and proportional growth, but with rapid urban development, urban expansion gradually replaces densification as the dominant pattern in cities (Sun et al., 2024). It is evident that as the urban population grows, it demands space to accommodate its economic, recreational or housing activities. For this reason, cities are concentrated centres of production, consumption, and waste disposal that drive land change and a host of global environmental problems (Grimm et al., 2008). Destruction of ecosystems, soil sealing, loss of biodiversity, alteration of the water cycle or regional climate modifications are some of the effects derived from the expansion of urban areas (Grimm et al., 2008; Kalnay and

E-mail address: imelendez@umh.es.

Cai, 2003; Rodríguez-Rojas and Grindlay Moreno, 2022).

One of the consequences of the increase in urban areas is the destruction of existing agricultural areas in the vicinity of the cities. These agricultural environments located close to cities represented a very important factor in the supply of food for the population, given their proximity to consumption centres. These areas have often been called agroecosystems, which are defined as communities of plants and animals interacting with their physical and chemical environments that have been modified by people to produce food, fibre, fuel and other products for human consumption and processing (Altieri, 2002). There is a clear tendency for the destruction of such agroecosystems due to various factors, but mainly due to the increase in the urban population that demands land for artificial uses, as well as the decreased profitability, as a consequence of the declining farm size, the water deficit and the increased water pollution (Martínez-Fernández et al., 2013).

Furthermore, from the point of view of urban morphology, traditional agroecosystems develop in the vicinity of built-up areas, with one use interspersed with another and generating a pattern of spatial heterogeneity due to the alternation of land covers. However, as the population increases, urban morphology evolves, modifying the initial urban morphology (He and Zhou, 2024). A marked process of homogenization of urban morphologies as the expansion of urban areas occurs is evident, resulting in a homogenization of the biotic and abiotic environment of urban areas and an enhancement of urban heat islands (Stuhlmacher et al., 2022).

1.1. Urban growth and UHI

One of the most significant environmental effects of urban expansion is the apparition of heat islands in such areas. Urban heat islands (UHI) are defined as the difference between the background rural and highest urban temperatures (Oke, 1973, 1976). The mechanisms that cause urban heat islands have been and are being studied by the scientific community to better understand how they work and to be able to adopt effective measures to minimize their impact. The origin of heat islands is due to the presence of materials of anthropogenic origin (e.g., concrete, pavement) that store more thermal energy than natural land covers (e.g., bare soil, vegetation) and may also reflect less sunlight, which together with heat sources of anthropogenic origin (e.g., internal combustion engines, heat rejected by air conditioning systems), the net effect is an increase in urban temperatures relative to nearby suburban and rural areas (Phelan et al., 2015). The intensity of UHIs is related to the size of cities (i.e., more intense heat islands can be expected in large urban areas), but also to density and the amplifying effect that urban sites have on each other (Li et al., 2020). In addition, changes in land use and the influence of local climate (e.g., winds, humidity) are factors that strongly influence the intensity of UHI (Zhou and Chen, 2018).

To mitigate the intensity of UHI, various strategies have been considered, such as, for example, the use of materials with higher albedo and/or emissivity, or increasing the areas with vegetation with solutions such as cool roofs, cool pavements, green roofs, and urban forestry (Phelan et al., 2015). These last solutions are considered in the field of Water Sensitive Urban Design and classified as Low Impact Development (LID), Green Infrastructure (GI), Sustainable Urban Drainage Systems (SUDS) or the Sponge City Concept (Sharma et al., 2019). They play a very important role, not only in mitigating UHI, but also in improving the urban water cycle or increasing urban biodiversity, among other benefits.

1.2. Agroecosystems for UHI mitigation

The presence of green spaces in cities is associated with social and health benefits for people (EEA, 2020). They also provide a set of ecosystem services, including environmental services (e.g., reducing elevated urban heat, pollution, flood mitigation, and offsetting greenhouse gas emissions), ecological services (e.g., providing habitats for urban wildlife and biodiversity conservation), and social and human health benefits (Paudel and States, 2023 and references therein). From the point of view of urban temperature regulation, green spaces, and especially those with trees or forests, are considered the most effective strategy for urban cooling primarily through shading and the reduction of ground surface temperatures, but in some cases through evapotranspiration as well (Saaroni et al., 2018). Urban green areas absorb heat, provide shade, and raise humidity that maintain surrounding surface and air temperatures and thus abate urban heat island effects (Jenerette et al., 2011).

It is important to consider that agroecosystems have a series of specific characteristics (herbaceous or tree crops, permanent or perennial crops, irrigation systems with surface or drip irrigation, etc.) that can influence their ability to regulate temperatures in their surroundings. Agroecosystems climate regulation is generated by the oasis effect of water evaporation, photosynthesis, and the provision of shade, which has an influence on convective and evapotranspiration processes (Albaladejo-García et al., 2020; Xu et al., 2017). In this sense, it has been identified that irrigated agriculture generates the so-called irrigation cooling effect (ICE) which has a great influence on summertime average daily daytime temperatures (Bonfils and Lobell, 2007). Additionally, shading by an adequate plant density and typology (primarily by tree crows), is a critical factor for temperature regulation and prevention of direct water evaporation (Boudjellal and Bourbia, 2018). Both, shading and irrigation, contribute to maintaining high soil moisture levels. This soil moisture is essential for local temperature regulation, and this capacity can be enhanced through landscape restoration and water harvesting measures in semi-arid agroecosystems (Castelli et al., 2019). Cooling, wetting and dimming effects, are irrigation induced effects that modify local climate in irrigation agroecosystems (Xu et al., 2017). Therefore, the availability of irrigation systems to maintain high soil moisture levels in urban-integrated agroecosystems can have a beneficial effect on mitigating UHI.

This last aspect is important to analyse from the perspective of water resource availability, given that a balance must exist between the ability to regulate temperature through the implementation of green spaces and water consumption. The act of planting vegetation in urban areas for the purpose of regulating temperature is an intentional modification of the ecosystem to provide ecosystem services (Jenerette et al., 2011). However, it creates a conflict between urban temperature regulation (ecosystem service) and water

consumption for evaporation. This would be considered an ecosystem disservice (Shackleton et al., 2016). It is therefore very important to consider the maintenance of traditional ecosystems, like palm groves in several semiarid/arid regions, which have adapted over centuries to existing climate and water (quantity and quality) availability. It is paradigmatic that enormous efforts and money are being invested in developing new green infrastructures in urban areas, which previously could have been occupied by areas that could fulfil comparable functions, such as traditional agroecosystems, which have been systematically eliminated in many urban areas.

Fortunately, it is still possible to find notable examples of traditional agroecosystems integrated within a modern urban framework, such as the case of the *Palmeral de Elche*, a North African oasis-type agroecosystem of medieval origin (Hernández et al., 2014; Larrosa Rocamora, 2003; Pablo Martínez and Pineda Pérez, 2003) that has survived to this day in southern Europe, and whose role in regulating urban temperature has not been previously studied systematically. Further research is needed into the functioning of traditional agroecosystems adapted to conditions with limited water resources, in order to assess whether they can contribute to mitigating urban heat islands in a manner comparable to recently created green areas, but with more efficient use of water resources and offering a greater diversity of ecosystem services.

This research aims to evaluate the influence of historical agroecosystems, such as the Elche Palm Grove, on urban temperature regulation. It is expected that traditional agroecosystems can play an important role in minimizing urban heat islands, hence the need for a better understanding of their integration in new urban areas to promote their conservation or restoration. It is important to know and compare their capacity to regulate urban climate concerning newly created green spaces since in cases such as palm groves, their adaptation to environmental conditions has been successfully modelled for centuries.

2. Material and methods

This section begins with a description of the study area. The fundamental characteristics of the satellite images used and auxiliary cartography are presented. The land cover class system used in this research is shown below. Finally, the statistical methods used in

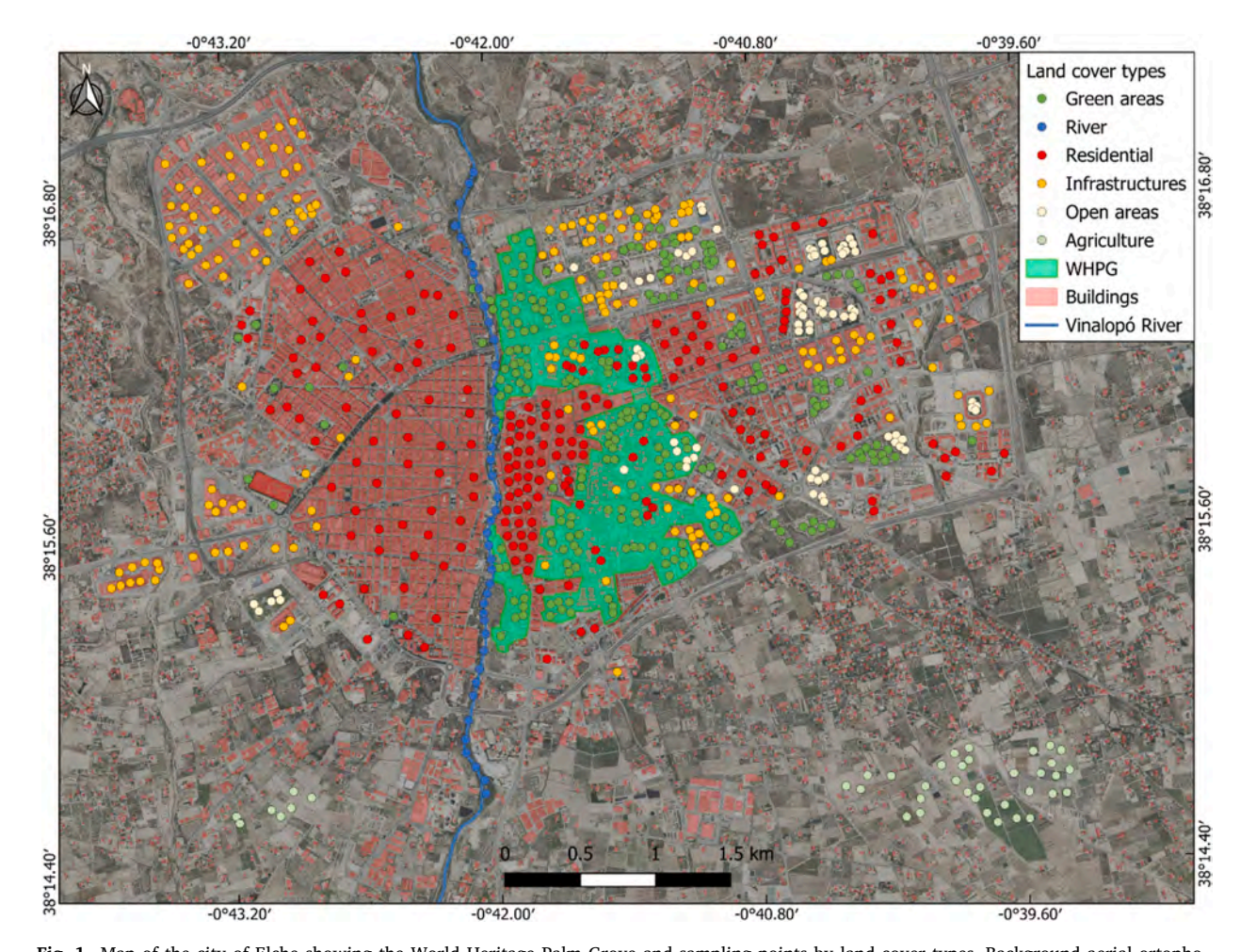


Fig. 1. Map of the city of Elche showing the World Heritage Palm Grove and sampling points by land cover types. Background aerial ortophotography is superimposed by the buildings as obtained by aerial LIDAR.

this manuscript are described.

2.1. Study area

Elche is a Spanish city located in the south of the province of Alicante (Valencian Community, Spain), with an approximate location at coordinates 38.16 N and 0.42 W. It is located 15 km from the Mediterranean coast and the city centre has a mean elevation of 85 m a. s.l. The Vinalopó River (Fig. 1) flows from north to south through the city centre. This watercourse and associated hydraulic infrastructure have conditioned the development and urban morphology of the city since its foundation in the Middle Ages. Elche climate is identified as semiarid Mediterranean. Köppen-Geiger climate class is *BSh* (hot semi-arid climate), with an annual average temperature above 18 °C and less than 300 mm of average precipitation (AEMET-IMP, 2011). Periods of severe drought contrast with events of very intense and dramatic floods. With a population of 238.285 inhabitants (INE, 2024), nowadays it is part of the ninth largest urban area (i.e., Alicante-Elche) of Spain (Gobierno de España, 2023).

The city is home to a relict agroecosystem, the *Palmeral de Elche*, formed by palm groves and its traditional irrigation system that dates back to medieval times. Date palm (*Phoenix dactylifera* L.) has long been one of the most important fruit crops in the arid regions of the Arabian Peninsula, North Africa, and the Middle East (*Chao and Krueger*, 2007) and whose cultivation spread to other regions such as the southeast of Spain. Cultivation of date palms in Elche is known at least since the Iberian times, dating around the fifth century B.C. (UNESCO, 2024).

The city has experienced significant population growth since the mid-20th century, with a significant conversion of traditional agroecosystems into other land uses, with the resulting soil sealing and associated environmental impacts (Navarro-Leblond et al., 2021). Fortunately, a large proportion of the urban area on the left bank of the Vinalopó River, where the historic centre of the city is located, is still occupied by palm groves. Most of the traditional date palm groves are rectangular plots bounded by single or double palms along the channels to generate a microclimate for hosting a wide array of associated crops such as *Medicago sativa* L. and *Punica granatum* L. inside, organized horizontally and vertically. This type of organization in the landscape has been described in the date palm garden cultivation in the Middle East (Tengberg, 2012).

Palm grove was possible by using Vinalopó River water resources for developing a complex irrigation system since the Middle Ages. This historic irrigation system was developed along the *Acequia Mayor* channel and fulfilled two tasks. Firstly, a set of perpendicular secondary channels (called *azarbes*) distributed water for irrigation of the palm grove and associated crops. And secondly, a system of watermills employed hydraulic energy for flour production (Melendez-Pastor et al., 2015).

The traditional palm groves, which are in a remarkable state of conservation and largely preserve the traditional irrigation system, constitute a relict agroecosystem in southern Europe that was recognized by UNESCO's World Heritage List in 2000 (UNESCO, 2024). World Heritage List recognizes the great diversity of the interactions between humans and their environment in order to protect living traditional cultural landscapes. With a total area of 507.4 ha and 181,138 registered palm trees according to the General Urban Plan of 1997, it is the largest palm grove of Europe (Ruiz-Navarro Ribalaygua, 2014). This study assesses the importance of the *Palmeral de Elche*, specifically the area considered as World Heritage Palm Grove (WHPG henceforth) by UNESCO, as an example of a historical agroecosystem with the capability for minimizing urban temperatures and reducing the intensity of UHI. In addition to the WHPG perimeter, and to assess its impact on the surrounding areas, a series of buffer zones were created at 100 m, 250 m, 500 m, and 1000 m. Points located outside these buffer zones were also analysed for comparative purposes.

Table 1
Satellite images and acquisition conditions. Air temperature, humidity and wind values obtained from an official meteorological station in Elche (MAPA, 2024).

$Image \ n^\circ$	Date of acquisition	Sensor	Temperature (°C)			Average relative humidity (%)	Average wind speed (m/s)	
			Average	Minimum	Maximum			
1	January 01, 2022	Landsat 8	10.1	5.1	19.1	91.0	0.58	
2	February 02, 2022	Landsat 8	13.7	6.3	25.8	56.8	0.91	
3	February 18, 2022	Landsat 8	13.3	5.4	22.3	72.6	0.77	
4	April 07, 2022	Landsat 8	16.8	7.9	25.3	55.7	1.32	
5	May 01, 2022	Landsat 9	18.9	12.4	25.2	66.8	0.92	
6	09/05/2022	Landsat 8	19.5	13.0	26.0	55.7	0.86	
7	17/05/2022	Landsat 9	22.0	15.2	28.0	73.4	0.94	
8	18/06/2022	Landsat 9	29.4	20.0	37.4	36.0	0.96	
9	26/06/2022	Landsat 8	23.4	16.0	28.7	73.4	1.13	
10	12/07/2022	Landsat 8	28.6	21.3	35.0	39.0	0.98	
11	05/08/2022	Landsat 9	29.5	23.9	35.3	49.4	1.1	
12	21/08/2022	Landsat 9	27.2	19.3	36.6	68.4	1.12	
13	30/09/2022	Landsat 8	19.7	16.1	26.8	56.6	1.42	
14	16/10/2022	Landsat 8	21.9	15.0	29.8	66.1	0.7	
15	01/11/2022	Landsat 8	21.9	17.2	29.7	78.5	0.72	
16	27/12/2022	Landsat 9	13.7	7.5	21.5	66.6	0.68	

2.2. Satellite images

This research used LST measurements obtained by medium spatial resolution satellites throughout the year 2022. Specifically, data acquired by the TIRS (Thermal Infrared Sensor) sensor on board the Landsat 8 satellite (Reuter et al., 2015) and the TIRS-2 (Thermal Infrared Sensor-2) sensor on board the Landsat 9 satellite (Eon et al., 2024) were used. Images acquired by both sensors were selected to provide a more frequent temporal repository. Before selecting the images, the atmospheric conditions were analysed based on the data available from an official meteorological station in Elche (MAPA, 2024), located on the southern outskirts of the city (38.248199N, -0.696059W). A total of 16 images were employed (Table 1) as they were acquired on days with low cloud cover and wind

Landsat 8 TIRS and Landsat 9 TIRS-2 Collection 2 Level-2 Science Products (Earth Resources Observation and Science Center, 2020) were employed for further analyses. LST products with 30 m of spatial resolution were obtained for the seventeen dates indicated in Table 1. These images were created with a single channel algorithm (band 10) jointly created by the Rochester Institute of Technology (RIT) and National Aeronautics and Space Administration (NASA) Jet Propulsion Laboratory (JPL) and are publicly available (USGS, 2024). Satellite images were obtained from the USGS EarthExplorer repository (https://earthexplorer.usgs.gov/). For each scene, a subset overlapping the study area was created and data values were converted to Celsius degrees.

2.3. Land cover classes identification

In order to evaluate temperature changes based on the characteristics of the study area's territory (e.g., vegetation or crop types, building types), the most relevant land covers were identified. The land cover classification hierarchy was based on the analysis of historical studies of the city of Elche and its World Heritage Site (Pablo Martínez and Pineda Pérez, 2003; UNESCO, 2024), as well as the researcher's prior knowledge of the study area (Hernández et al., 2014; Melendez-Pastor et al., 2015; Navarro-Leblond et al., 2021).

A total of six land cover types were identified within the city, as well as in its immediate agricultural environment (to compare urban temperature with the rural environment): green areas, rivers, residential areas, infrastructure, open spaces, and agriculture. This generic categorization was divided into several more specific categories, identified as land cover classes, for a total of 17 land cover classes, as detailed in Table 2 (the table also includes a description and illustrative image of each class). The purpose of this hierarchical classification of land cover types and classes was to allow for a more in-depth analysis of LST changes according to different levels of categorization specificity.

A georeferenced database of land covers was created using a Geographic Information System (GIS), in this case QGIS (CITA). A stratified random sampling of points was conducted within the urban environment, defined based on building maps available from the National Geographic Institute of Spain (URL: www.ign.es) and palm groves cartography (UNESCO, 2024). In addition, an irrigated agricultural area located outside the city was used for temperature comparison. The main land covers in the study area were identified through aerial photographs and field reconnaissance. High-resolution, up-to-date georeferenced aerial photographs from the National Plan for Aerial Orthophotography of the National Geographic Institute of Spain (URL: https://pnoa.ign.es) were used. In total, land covers were sampled and identified for a total of 799 locations or sampling points (Table 2).

Each of the land cover sampling points was identified as included or not within the UNESCO World Heritage Palm Grove (Table 2). To assess the potential differential influence of the WHPG on urban temperature regulation, the study area was zoned with various influence bands around it. Four buffer zones were established around the perimeter of the WHPG, with the following distances of increasing size selected: 100 m, 250 m, 500 m, and 1000 m. This allowed us to assess changes in LST between sampling points located within the WHPG, points located within each of the buffer zones, and finally, points that were further than 1 km from the WHPG.

2.4. Statistical methods

Statistical analyses were performed for a database with a total of 12,784 LST measurements (i.e., 799 sampling points and 16 different dates of image acquisition). In order to determine the influence of the different land covers or the agroecosystems of the WHPG of LST measurements, five different factors were used individually or combined, namely: 1) image number, corresponding to the date of acquisition of the satellite images according to Table 1; 2) land cover types as specified in Table 2; 3) land cover classes as a more detailed analysis of land cover presents in the study area (see Table 2); 4) the ubication of the sampling point within the WHPG or outside it (buffer zones); and 5) the comparison of the traditional agroecosystems, mainly located within the WHPG perimeter respect to other urban green areas. The following statistical test were computed each of the four factors (induvial or combined) in order to determine the influence seasonal changes, land cover classes and position of the sampled within or outside the WHPG on LST.

The first stage of each statistical analysis was the computation of descriptive statistics in order to gain knowledge of LST variations through the study period. Numerical summaries of descriptive statistics for the four above-mentioned factors were developed. Mean, standard deviation (St.Dev.), minimum (Min.), maximum (Max.) and the coefficient of variation (CV) statistics were computed for all the samples and factors. After that, data distribution was analysed in ordert to evaluate whether they adopted a normal distribution or not. The Lilliefords' test (Lilliefors, 1967) was applied to the different datasets and it revealed that they did not adjusted to a normal distribution in any of the cases. For this reason, non-parametric tests were applied for further analyses.

The effect of individual factors on LST measurements was also analysed in the following way. The effect of time, land cover type, land cover class and ubication of the sampling points respect to the WHPG on the mean LST values was analysed with the Kruskal-Wallis test (Kruskal and Wallis, 1952). It was used to perform the comparison between the means (i.e., influence of the factors

Table 2
Description of the land cover types and classes used in the study. Number of sampled locations and those inside the WHPG are detailed. An illustrative image for each land cover class is included too.

Land cover type	Land cover class	Description	Sampled points	Inside WHPG	Photo
Green areas	1	Traditional palm grove. The traditional irrigation system is evidenced and used for the maintenance of the palm trees.	116	82 (70.7%)	
Green areas	2	Gardens with palm trees.	71	52 (73.2%)	
Green areas	3	Other type of gardens.	47	2 (4.3%)	
River	4	Artificial riverbed. This portion of the Vinalopó River is channelled.	28	0 (0%)	
River	5	Vegetated riverbed. This portion of the Vinalopó River is not channelled. River margin vegetation predominantly includes Tamarix sp. and Phragmites sp.	14	0 (0%)	
Residential	6	Old town. Historic city centre, with an urban structure of medieval origin.	49	0 (0%)	
Residential	7	Compact residential. Urban areas developed since the mid-20th century.	78	0 (0%)	
Residential	8	New residential. Urban areas developed since the beginning of the 21st century.	52	0 (0%)	
Residential	9	Houses with gardens. Single-family homes with plots that include gardens and often individual swimming pools.	32	19 (59.4%)	

Land cover type	Land cover class	Description	Sampled points	Inside WHPG	Photo
Infrastructures	10	Endowments. Includes schools, university buildings, hospitals, etc.	68	10 (14.7%)	
Infrastructures	11	Shopping centres.	19	0 (0%)	1214
Infrastructures	12	Industrial buildings.	60	1 (1.7%)	
Infrastructures	13	Parking lots.	53	5 (9.4%)	
Open areas	14	Sports-Natural grass.	23	0 (0%)	
Open areas	15	Sports-Artificial grass.	18	0 (0%)	
Open areas	16	Weedy open fields. Undeveloped plots occupied by herbaceous vegetation	31	10 (32.2%)	
Agriculture	17	Peri-urban field crops.	40	0 (0%)	

levels on LST values). Independent analyses were performed for each of the four previous factors (i.e., image number, land cover type, land cover class, ubication respect to the WHPG). Next, in each of the four previous types of analysis, the Dunn test (Dunn, 1964) was applied for pairwise comparisons of the samples. This allowed the identification of homogeneous subgroups of LST measurement.

The combined effect of individual factors on LST measurements was analyses too. To compare the joint effect of time (image number factor) and the constituents of the urban structure (i.e., land cover type, land cover class and WHPG factors), the Friedman rank test (Friedman, 1937) was applied. This test revealed whether there were significant differences in the LST measurements

combining two factors. Time vs. land cover type, time vs. land cover class, time vs. WHPG buffer zones, and time vs. green areas were the combinations of factors employed in the analyses.

All statistical analyses and figures were developed with the R programming language (R Core Team, 2023).

3. Results

The results of the research are presented structured according to the factors analysed in the different statistical tests. First, the results are shown considering the time factor (date of image acquisition), used to analyse seasonal changes in LST. Next, the results obtained considering the land cover factors identified (types and classes, according to the classification hierarchy used), used to evaluate the influence of the different land covers on LST, are presented. Finally, the thermal regulation capacity of the WHPG is evaluated, both within its perimeter and in its surroundings (buffer zones), and the changes in LST between the traditional agroecosystem and other green areas are compared.

3.1. LST temporal variability

Significant differences in LST values between the different dates of satellite image acquisition (p-value <0.001 in the Kruskal-Wallis test) were observed. The LST measurements for the available images (Table 3 and Fig. 2) followed a constant growth from January to June (images 1 to 8), going from an average value of about 15 °C to a value of 48 °C. During the summer months (June to August) high temperatures were maintained (averages of more than 39.5 °C), although without reaching the average of the first image of June (06/18/2024). During the last third of the year, temperatures decreased noticeably below the annual mean LST (dashed horizontal line on the violin graph).

Both in the standard deviation data in Tables 3 and in the graphs in Fig. 2, greater variability of LST measurements was observed for the spring months (images 4 to 7), compared to the rest of the year. LST observations for May exhibited standard deviation values higher than 3 °C, which doubled the value for January or December.

After performing the Dunn test, homogeneous subgroups of images were established, whose LST values are similar to each other. These subgroups show the similarities in the LST measurements for the February and December images (subgroup a), as well as between various spring-autumn images (subgroup b), or images close to each other from a temporal point of view (subgroups c, d, e, f).

3.2. Land covers and LST

Significant differences in LST values between the different land cover types were observed (p-value <0.001 in the Kruskal-Wallis test). Lower annual LST values (Table 4) were reported for green areas (mean= $31.4\,^{\circ}$ C; CV= $32.4\,^{\circ}$) and the river (mean = $31.3\,^{\circ}$ C; CV= $31.4\,^{\circ}$). On the contrary, the highest values were reached for the infrastructure land cover type category (mean= $34.9\,^{\circ}$ C; max.= $58.2\,^{\circ}$ C). Agricultural areas located on the urban periphery recorded intermediate LST values (mean = $32.8\,^{\circ}$ C) but quite a high-temperature variability (CV = $32.6\,^{\circ}$).

Several homogenous subgroups were identified with the post hoc analysis (Fig. 3, Table 4). The first subgroup (identified with the letter a) included green areas and river land cover types. It is associated with the lowest average temperature sampling points. On the contrary, subgroup d is associated with the highest average temperatures. Infrastructures land cover type is uniquely included in group d while open areas exhibit a more variable LST behaviour. Subgroups seem to be related to decreasing average LST values in the following order: d > e > c > b > a.

For a more detailed analysis of LST in the study area, urban temperatures were analysed for each of the seventeen land cover classes (Fig. 4). Land cover classes 1 (*Traditional palm grove*), 2 (*Gardens with palm trees*) and 5 (*Vegetated riverbed*) exhibited great similarity among them. Lower average LST values than the rest of the land cover classes were recorded. Land cover classes 17 (*Agricultural areas*), 3 (*Other type gardens*), 4 (*Artificial riverbed*), 16 (*Weedy open fields*) and 9 (*Houses with gardens*) were also below the average LST value of the study (dashed line in the boxplot). On the contrary, higher average LST values were observed for land cover classes 11 (*Shopping centres*), 12 (*Industrial buildings*) and 15 (*Sports-Artificial grass*).

Finally, the Friedman rank sum test was used to analyse the joint effect of two factors on LST measurements. Two different analyses were performed: a) the combinations of factors time (date of acquisition of the images) vs land cover type (i.e., the six broad categories of land covers; see Table 2); and b) the combinations of factors time (date of acquisition of the images) vs land cover class (i.e., the seventeen land cover classes identified in table 2). Significant differences in LST measurements were observed for the pair of factors time | land cover type (p-value <0,001). Also, significant differences in LST measurements were observed for the pair of factors time | land cover classes (p-value <0,001). Regardless of how general (land cover type) or more specific (land cover class) the classification hierarchy has been developed, the variation of LST over time is shown to be highly affected by the composition of the territory, even for a medium-sized city such as Elche.

3.3. Influence of the WHPG and the traditional agroecosystem on temperature regulation

The next step in the research was to determine whether the current structure of the WHPG presents temperature differences with respect to the rest of the city. Furthermore, it is necessary to understand the specific effect of the traditional agroecosystem on urban temperature regulation, specifically in comparison to land cover classes with a significant amount of vegetation.

A total of 182 sampling points were located within the WHPG (Table 5). Land cover classes identified for these sampling points

were mainly 1-Traditional palm grove (82 sampling points), 2-Gardens with palm trees. (52 sampling points). Five buffer zones, at 100m (75 sampling points), 250 m (73 sampling points), 500 m (77 sampling points) and 1000 m (139 sampling points), were employed to determine the thermal regulation influence of the WHPG in the surroundings. A sixth buffer zone was for the points farther than 1 km from the WHPG perimeter.

Mean average annual LST increased from inside the WHPG thorough the different buffer zones and outside them (Table 5 and Fig. 5). The average temperature throughout the year was approximately $3.5\,^{\circ}$ C lower within the WHPG perimeter than in the area outside the buffer zones (distances greater than 1 km). While minimum LST was similar inside the WHPG and outside it ($13.2\,^{\circ}$ C and $13.5\,^{\circ}$ C respectively), a large difference in maximum temperatures was observed. Up to $7.9\,^{\circ}$ C of difference was observed by comparing the maximum temperatures reached within the WHPG ($50.3\,^{\circ}$ C) respect to outside this protected palm grove ($58.2\,^{\circ}$ C). This is largely due to the difference in soil cover between the protected agroecosystem in the WHPG and that in other areas of the city (e.g., densely populated areas, commercial zones, industrial zones).

Kruskal-Wallis test revealed significant differences in LST values among the different buffer zones (p-value < 0.001).

Several homogenous subgroups were identified with the post hoc analysis (Table 5 and Fig. 5). The first subgroup (identified with the letter a) included the WHPG and the immediate 100 m buffer zone. It is associated with the lowest average temperature sampling points. A second subgroup (b) included all the four buffer zones while the sampling points of the study area outside the last buffer constituted a separate subgroup (c). Friedman rank sum test allowed the analysis of significant differences of LST with respect to the factors of time (date of acquisition of the images) and the buffer zones. Significant differences in LST measurements were observed for this pair of factors (p-value <0,001).

Finally, temporal changes in LST were specifically analysed for land covers considered as green areas. These included land cover classes LC1-Traditional palm grove, LC2-Gardens with palm trees, and LC3-Other type of gardens. Sampling points of the same land cover class located inside or outside the WHPG were analysed independently. A total of 234 sampling points was employed at these stage of the analyses (Table 6). There were no LC3 sampling points within the WHPG perimeter.

The average annual LST was below 32 $^{\circ}$ C for green areas located within the WHPG, and lower for the LC2 land cover class. This type of green area also had the lowest annual maximum temperature, although its coefficient of variation was the highest of the five green area classes studied. Kruskal-Wallis test revealed significant differences in LST values among the different green areas (p-value <0.001). Three homogenous subgroups were identified with the post hoc analysis (Table 6 and Fig. 6). The first two subgroups (identified with the letters a and b) were representative of the Traditional palm grove within or outside the WHPG respectively. The third subgroup (c) was associated to LC2-Gardens with palm trees located within the WHPG perimeter.

Friedman rank sum test revealed significant difference of LST with respect to the factors of time (date of acquisition of the images) and the different green areas (p-value <0,001). In this regard, Fig. 6 shows the temporal evolution of LST recorded in each of the 16 satellite images for the five types of green areas analysed. Sampled locations within the WHPG area are represented by green triangles and grey circles for points located outside the WHPG perimeter.

The temporal evolution of LST for LC1-Traditional palm grove shows a very similar temporal pattern both inside and outside the WHPG (Fig. 6). Since the management and irrigation system are the same for both types of green areas, this agroecosystem presents a very stable thermal regulation capacity in the studied area. On the other hand, notable differences are observed in the temporal evolution of LST for LC2-Gardens with palm trees depending on their location inside or outside the WHPG perimeter. These green areas contain palm trees but do not have the structure or elements characteristic of a palm grove-type agroecosystem. They have varying amounts of palm groves, interspersed with other types of trees and lawns, and therefore require much more water for maintenance.

Finally, the green areas in the LC3-Other type of gardens category are parks developed within the urban fabric, with relatively small dimensions, varying presence of trees and lawns, and a large amount of sealed soil (sidewalks or children's play areas).

Table 3Descriptive statistics and Dunn's test homogeneous subgroups considering the date of satellite image acquisition as factor.

Image	Date	Mean	St.Dev.	Min.	Max.	CV(%)	Subgroups
1	January 01, 2022	15.24	1.43	13.23	22.46	9.4	_
2	February 02, 2022	18.51	1.64	15.69	25.76	8.8	a
3	February 18, 2022	22.24	1.88	18.68	30.04	8.5	
4	April 07, 2022	27.60	2.72	23.30	39.12	9.9	b
5	May 01, 2022	35.26	3.08	29.88	45.76	8.7	c
6	09/05/2022	35.74	3.45	29.51	47.68	9.6	c
7	17/05/2022	38.49	3.01	32.53	50.61	7.8	d
8	18/06/2022	48.35	2.48	42.35	56.94	5.1	
9	26/06/2022	39.51	2.24	33.48	47.48	5.7	d
10	12/07/2022	44.82	2.23	39.03	54.38	5.0	e
11	05/08/2022	47.95	2.52	41.11	58.23	5.3	
12	21/08/2022	44.05	2.27	37.75	53.15	5.2	e
13	30/09/2022	28.41	2.17	24.83	36.47	7.6	b, f
14	16/10/2022	32.33	2.19	28.26	41.42	6.8	
15	01/11/2022	29.78	1.95	26.33	38.30	6.6	f
16	27/12/2022	19.06	1.49	16.69	25.06	7.8	a

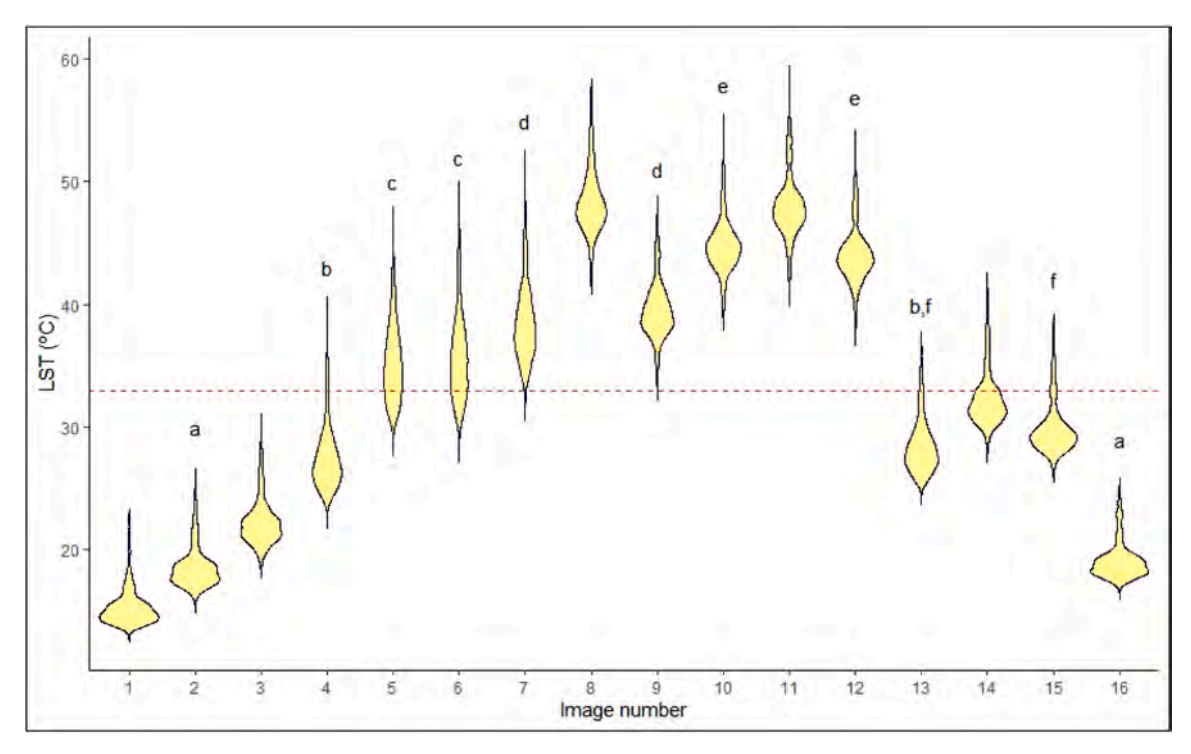


Fig. 2. Violin plot of satellite LST measurements for the different images. Dunn's test homogeneous subgroups are identified with letters. Horizontal dashed line represents average annual LST for the entire study area.

Table 4Descriptive statistics of annual LST for the six land cover types. Dunn's test homogenous subgroups are indicated with letters.

Туре	Mean	St.Dev.	Min.	Max.	CV(%)	Subgroups
Green areas	31.41	10.17	13.23	50.34	32.4	a
River	31.32	9.83	13.65	48.71	31.4	a, b
Residential	32.84	10.60	13.38	51.24	32.3	c
Infrastructures	34.93	10.86	13.59	58.23	31.1	d
Open areas	33.94	10.45	14.48	55.24	30.8	c , d, e
Agriculture	32.77	10.68	14.45	53.45	32.6	b , c, e

4. Discussion

Concern about the effects of high temperatures and heat waves on the population, especially among the most vulnerable (Mazzone et al., 2023; Newsome, 2023), and their intensification in urban environments is a matter of great importance (Hsu et al., 2021; Huang and Cadenasso, 2016). It is clear that the population of cities is more exposed to the effects of high temperatures and their strategies to cope with them depend largely on their age, health status and socioeconomic conditions. This causes numerous people to die each year from this cause (Ballester et al., 2023; Cuerdo-Vilches et al., 2023), making it a major cause for social concern. This is why urban managers and planners, the scientific community and the general population must ask themselves how to improve cities from the point of view of climate comfort, especially considering the growing trend of urban population growth.

One of the areas of the planet with great concern about the effects of heat waves on the urban population is the Mediterranean basin. Recent studies have shown that in the European context, the highest risks of heat-related mortality were observed in countries near the Mediterranean Sea in all sex and age groups, with generally higher values for older adults (Ballester et al., 2023). In this sense, the study area is characterized by a semi-arid Mediterranean climate with maximum summer temperatures that frequently exceed thirty-five degrees. This was the case in the summer of 2022, which was characterized by very intense heat waves that extended through the southwester of Europe (Copernicus, 2022). Maximum daily air temperature (Table 1) during the studied period was equal to or greater than 35 °C during four of the 16 analysed days, and 28 °C on half of the study days. This reiteration of episodes with high temperatures is becoming more and more frequent in the study area and in fact, coincided with days with satellite images, as is the case of image 8 (date 06/18/2022), which corresponds to an acute heatwave (AEMET, 2022). This temporal coincidence provides very valuable information on the dynamics of LST in the study area during particularly intense heat episodes.

This scenario of high temperatures during the study period has been reflected in the observation of significant differences in

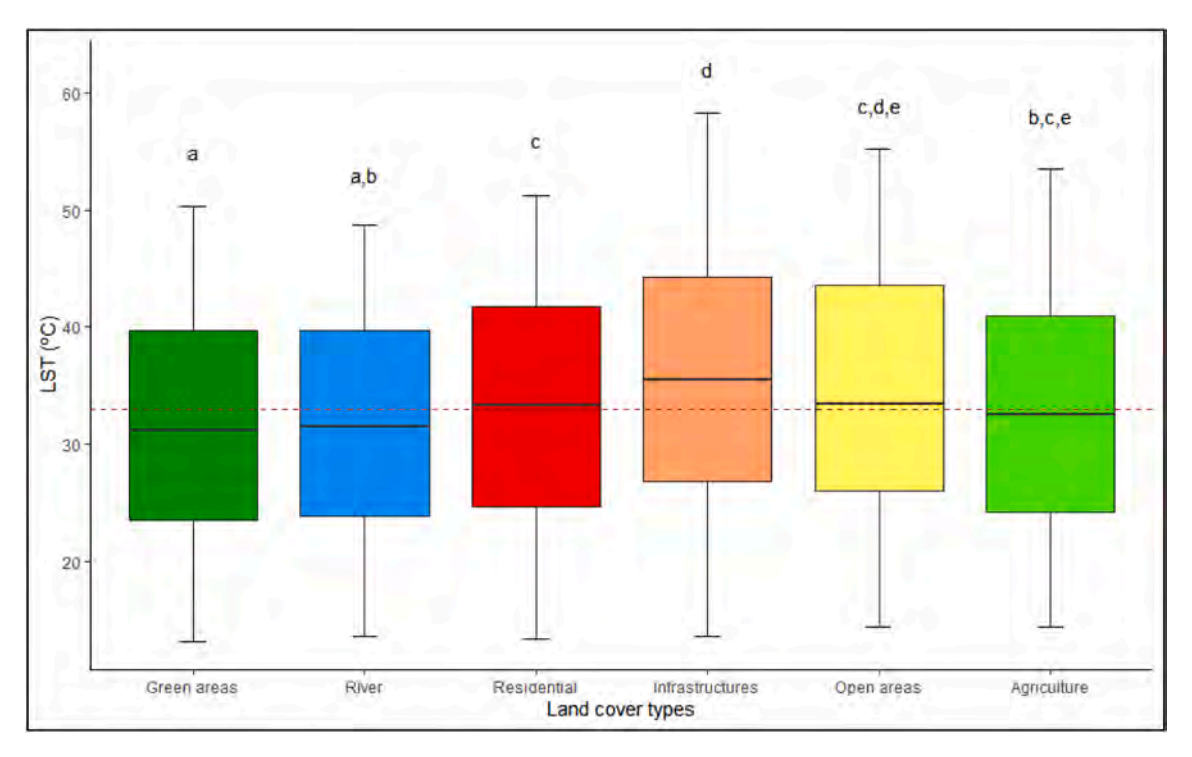


Fig. 3. Boxplot chart of LST for the different land cover types. Dunn's test homogeneous subgroups are identified with letters. Horizontal dashed line represents average annual LST for the entire study area.

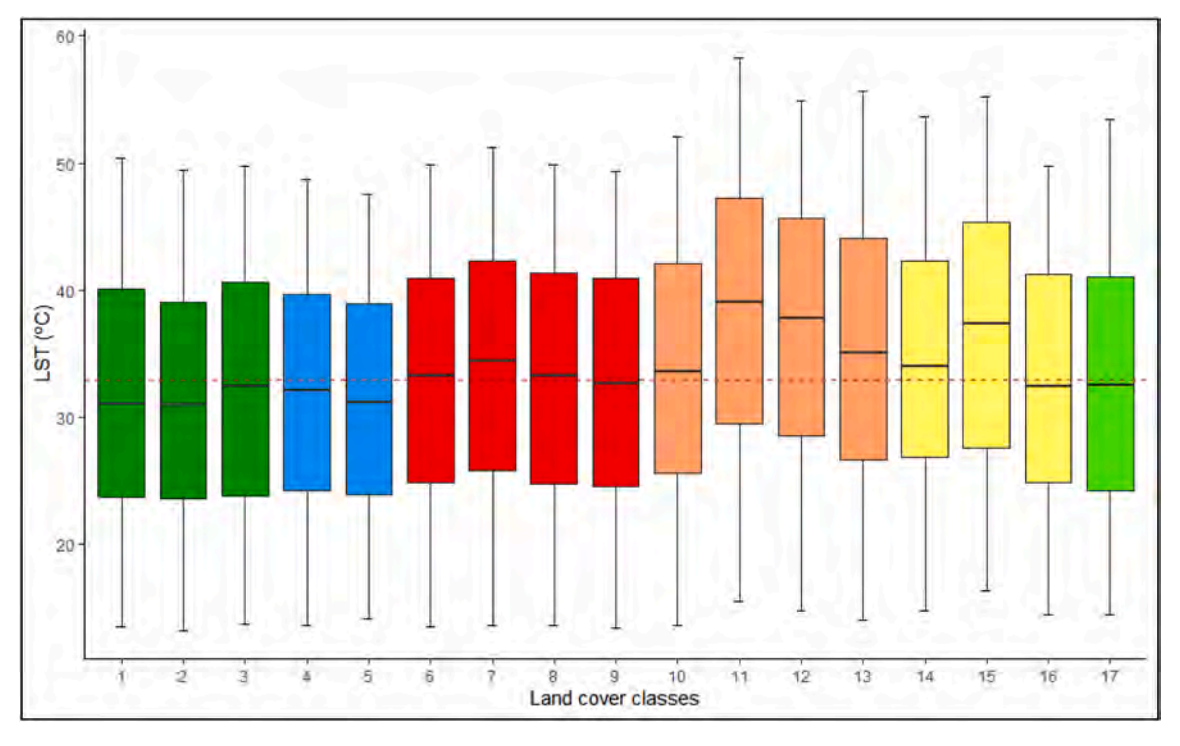


Fig. 4. Boxplot chart of LST for the different land cover classes. Dunn's test homogeneous subgroups are identified with letters. Horizontal dashed line represents average annual LST for the entire study area.

Table 5
Descriptive statistics of annual LST for the zoning of the study area with buffers. Dunn's test homogenous subgroups are indicated with letters.

Buffer zone	Sampling points	Mean	St.Dev.	Min.	Max.	CV(%)	Subgroups
WHPG	182	31.19	10.18	13.23	50.34	32.6	a
100 m	75	32.05	10.35	13.46	49.45	32.3	a,b
250 m	73	32.64	10.45	13.59	49.80	32.0	b
500 m	77	32.58	10.34	13.81	50.56	31.7	b
1000 m	139	33.06	10.45	13.77	54.73	31.6	b
Out of buffer	253	34.65	10.87	13.67	58.23	31.4	c

temperatures between the different types/classes of land covers and dates. Friedman rank sum test revealed this joint effect of land cover (type or class) and time (date of acquisition of the images) on LST measurements. Over the last decades, the enormous impact that different types of soil cover have on the temperatures observed in cities and on the development of UHI (Aram et al., 2019; Huang and Cadenasso, 2016; Yang et al., 2024) has been demonstrated. This is undoubtedly related to the presence of material of anthropic or artificial origin, with a thermal behaviour very different from that of natural materials, which together with the possible existence of heat sources (e.g., air conditioning systems in buildings), the net effect is an increase in urban temperatures relative to nearby suburban and rural areas (Phelan et al., 2015). In addition to the obvious and expected higher temperatures in areas with residential buildings, shopping centres or industrial zones (Fig. 7), the effect of artificial turf for sports fields on urban temperature was very noticeable. Located far from the most densely populated areas, it is evident that they constitute hotspots of high temperatures. Its influence on the local microclimate seems to be evident. Recent studies are focusing on the impact that surfaces occupied by artificial turf have on the temperature of cities, especially in areas potentially used by at-risk populations such as children (Namazi et al., 2024). In this sense, initiatives are beginning to be developed to minimize their thermal impact on the urban water cycle (van Huijgevoort et al., 2024). The use of artificial grass has become widespread due to its robustness and the fact that it does not require the same water consumption as natural grass, but it is undoubtedly necessary to continue developing products and systems that do not generate the current pollution problems (de Haan et al., 2023) and do not negatively alter the urban water cycle and urban temperatures.

The ability of green areas to mitigate UHI is widely known and used in urban planning (Kim et al., 2024; Li et al., 2024). In addition to providing recreational areas for the population, they can attenuate the temperatures reached during the warmest months. The presence of trees and their spatial arrangement (Jayasinghe et al., 2024) are key to this temperature-regulating effect. However, their implementation is not equally simple in all urban areas, given that their maintenance may involve the provision of huge quantities of water (Guo et al., 2021) that are not easily provided in arid and semi-arid areas. It is necessary to evaluate and implement strategies for the mitigation of heat islands, but trying to adopt sustainable, long-lasting solutions preferably with the capacity to improve other critical aspects in cities such as the urban water cycle. In this sense, the implementation of new green infrastructures or the

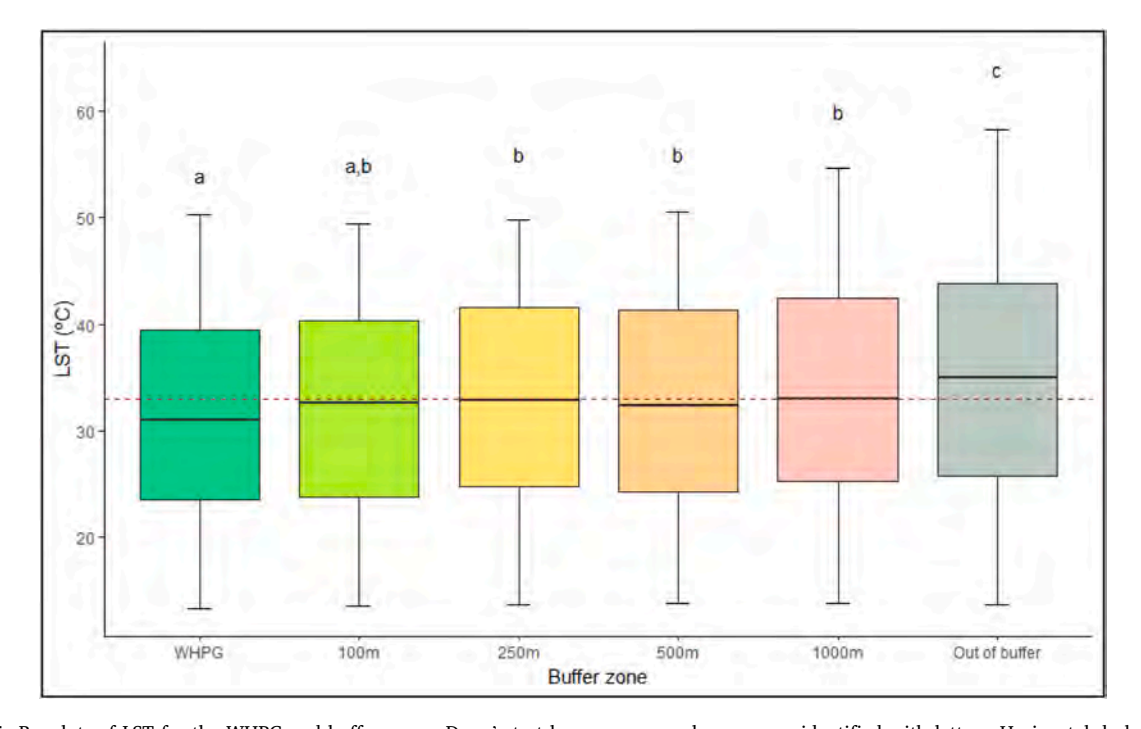


Fig. 5. Boxplots of LST for the WHPG and buffer zones. Dunn's test homogeneous subgroups are identified with letters. Horizontal dashed line represents average annual LST for the entire study area.

Table 6
Descriptive statistics of annual LST for the different green areas, within and outside the WHPG. Dunn's test homogenous subgroups are indicated with letters.

Land cover class	WHPG	Sampling points	Mean	St.Dev.	Min.	Max.	CV(%)	Subgroups
LC1	Inside	82	31.18	10.10	13.45	50.34	32.4	a
	Outside	34	32.81	10.44	13.97	49.23	31.8	b
LC2	Inside	52	29.83	9.88	13.23	48.08	33.1	c
	Outside	19	32.42	10.27	13.82	49.36	31.7	a,b
LC3	Outside	47	32.26	10.17	13.71	49.80	31.5	a,b

conservation of historical systems that allow similar functionality (like traditional agroecosystems such as the *Palmeral de Elche*) should be a priority in urban planning.

Traditional date palm groves are agroecosystems adapted to conditions of high temperatures and low availability of water resources (Chao and Krueger, 2007; Krueger, 2021; Tengberg, 2012). It is even possible that date palms are grown using low-quality water (high salinity) for their maintenance, which would limit the growth of many plant species (Hernández et al., 2014; Lalouani and Alkama, 2012). For this reason, integrating the palm groves' grids within the urban environment is essential for the long-term sustainability of urban development in arid environments (Matallah et al., 2023). From the point of view of this study, it is possible to see how the areas occupied by the WHPG have lower temperatures and are a cooling hotspot for the surrounding areas (Fig. 7). Analysis of the buffer zones around the WHPG has shown a very noticeable upward thermal gradient from within the WHPG to the surrounding area. The temperature in the first 100 m around the WHPG is similar to that within the protected perimeter (see Table 5 and Fig. 5) and increases progressively thereafter, with no apparent thermal regulating effect beyond 1 km. This cooling effect is due in part to the presence of vegetation and the shading it generates, but also to traditional irrigation infrastructures with open canals on the surface. Thus, the shading, transpiration and evaporation mechanisms contribute to this control of urban temperature by

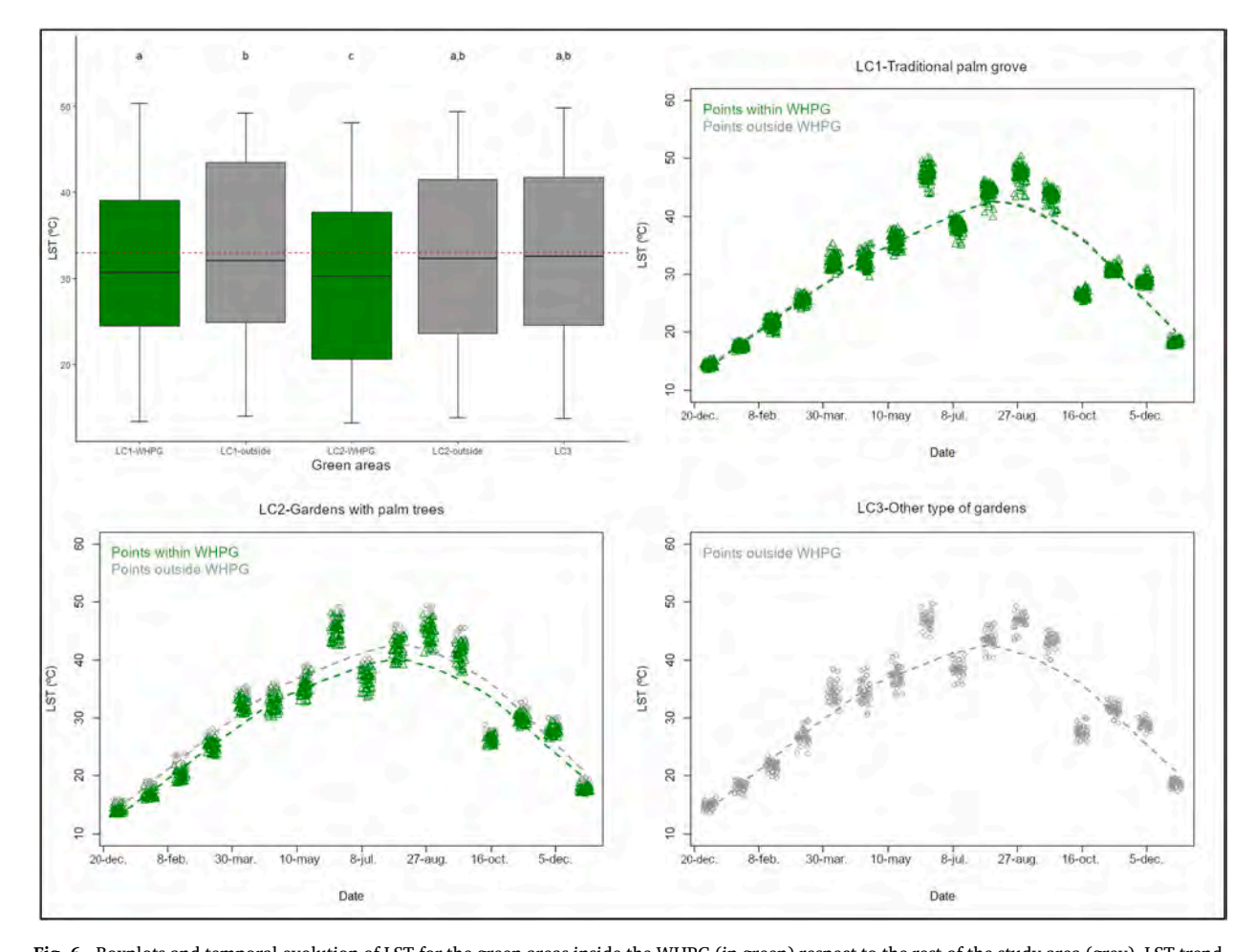


Fig. 6. Boxplots and temporal evolution of LST for the green areas inside the WHPG (in green) respect to the rest of the study area (grey). LST trend lines are included. Dates corresponds to the acquisition time of employed satellite images.

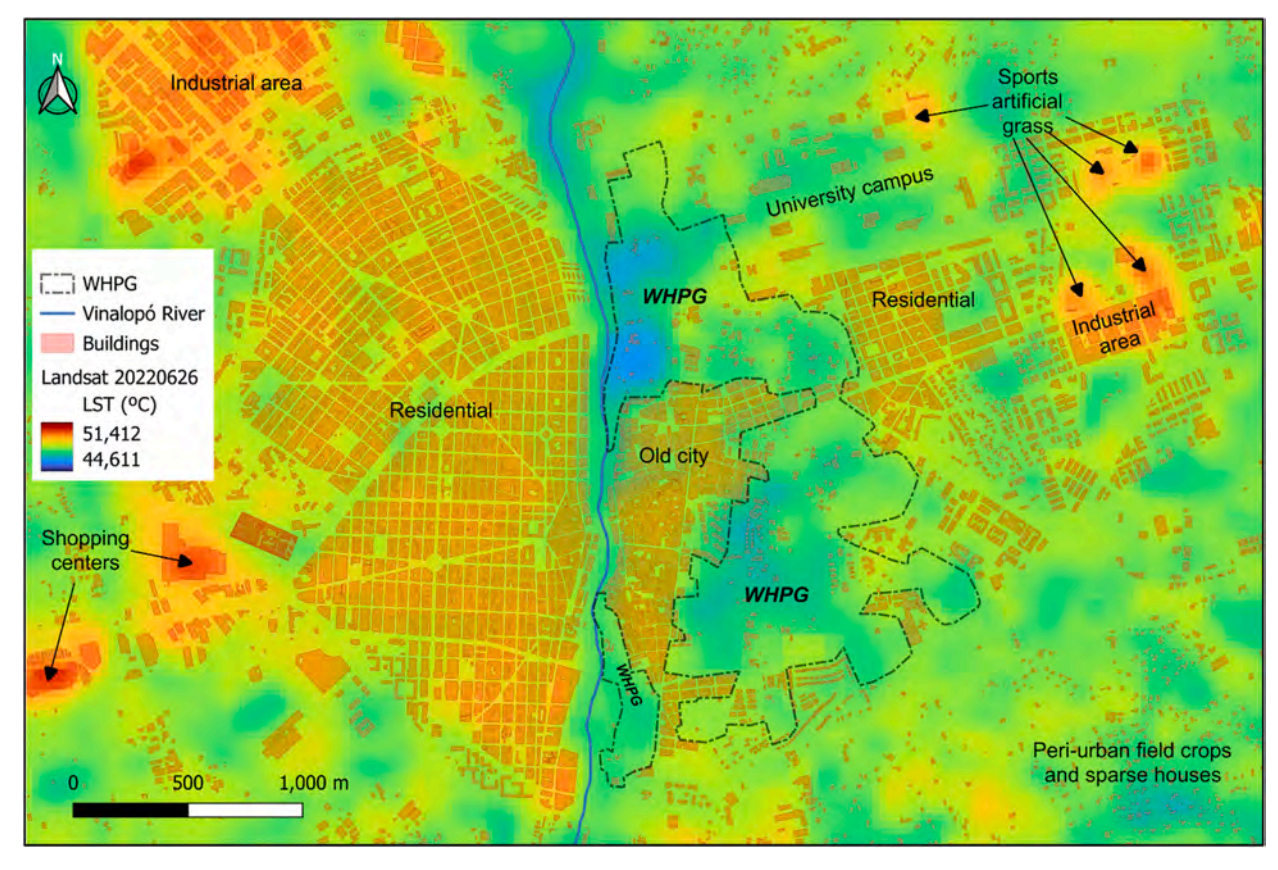


Fig. 7. Spatial distribution of LST for the heatwave of June 26, 2022.

the traditional palm groves (Boudjellal and Bourbia, 2018; Matallah et al., 2023). But, in addition to the presence of urban green spaces as a strategy to minimize UHI, it must be taken into consideration that the homogenization of cities can negatively affect temperature control. The increase in shape compactness (i.e., infill) and shape complexity (i.e., sprawl) have been reported as factors that may increase the intensity of daytime surface UHI (Stuhlmacher et al., 2022). Urban form explains up to 70 % of LST inequality in European cities and factors such as the equal distribution of impervious surfaces need to be addressed in urban planning (Mashhoodi and Unceta, 2024).

It is clear that urban planning can substantially improve the thermal comfort of the population and make urban environments more habitable (Hsu et al., 2021; Li et al., 2024). From the point of view of temperature regulation through green infrastructure, it is necessary to adopt effective solutions that are also rational about the consumption of water and other resources. In this sense, the traditional oasis landscape appears to offer a true cooling strategy suitable for mitigating heat effects and to reduce the summer cooling loads in the residential sector (Boudjellal and Bourbia, 2018). With respect to the case study of this research and considering the blue-green system definition (Probst et al., 2022), the WHPG could be considered a good example of it, due to its strategic development process, a great impact on urban temperature regulation and the ecosystems services that provide among others. It is evident that the type of green area (traditional agroecosystem or recently created urban parks) have different thermal regulation capacities (Table 6 and Fig. 6), as well as different water consumption depending on the type of vegetation present, and that should be taken into account for adaptation to climate change. Efforts to conserve and enhance traditional agroecosystems, adapted for centuries to arid and semi-arid climates, must be taken into consideration by authorities and urban planners to achieve better future urban development.

Regarding the limitations of this study, further research is needed in different areas. First, it is important to better understand the effects of urban morphology and that of the traditional agroecosystem on urban temperature regulation. It is necessary to investigate the influence of the spatial configuration of the agroecosystem in relation to the physical environment (land morphology, river channel layout) and the urban environment (building height, street orientation relative to prevailing winds). Geometry and material makeup of "urban canyons" may intensify pedestrian thermal stress in the daytime and adversely affecting nighttime cooling as well (Pearlmutter et al., 2009). Furthermore, it is necessary to quantify the ecosystem services and benefits of the different green areas, primarily in relation to their water consumption. Irrigation of green areas is essential for their maintenance and produces a cooling effect, but it is necessary to quantify the differences in water consumption between the agroecosystem and other types of green areas. Finally, the study has a one-year time frame, so it would be interesting to extend the study period and compare the functioning of the Elche Palm Grove with other similar types of agroecosystems.

5. Conclusions

This research advances the understanding of the role of traditional agroecosystems in urban temperature control. These types of systems have been systematically eliminated to convert them into built-up areas or, in the best of cases, into green areas, often not designed with sustainability criteria from the point of view of water consumption. In arid and semi-arid areas, palm groves (such as the *Palmeral de Elche*) can be a very important solution to mitigate the high temperatures reached in cities.

The capacity of these traditional palm grove-type agroecosystems to minimize urban heat islands has been demonstrated in this study, even during episodes of very intense heat waves. Their ability to integrate into the urban fabric, providing temperature regulation in its perimeter and surroundings, heterogeneity to the landscape and using water resources of undesirable quality for many crops, makes them highly interesting in urban planning. Their conservation or recovery must be a priority, not only for their cultural and historical value but also for the environmental benefits they provide.

The methodology presented, based on the study of surface temperature using remote sensing, can be extrapolated to other study areas. It is necessary to continue advancing in the understanding of urban morphology and the arrangement of the different elements that make up the urban fabric, to optimize temperature attenuation strategies, promoting the presence of green areas and/or traditional agroecosystems, but always with the perspective of seeking water-sensitive solutions.

Ethical Statement for Remote Sensing Applications: Society and Environment

Hereby, I Ignacio Melendez-Pastor consciously assure that for the manuscript *Traditional agroecosystems for urban temperature* regulation: a remote sensing analysis of an historical palm grove the following is fulfilled.

- 1) This material is the author' own original work, which has not been previously published elsewhere.
- 2) The paper is not currently being considered for publication elsewhere.
- 3) The paper reflects the author' own research and analysis in a truthful and complete manner.
- 4) The results are appropriately placed in the context of prior and existing research.
- 6) All sources used are properly disclosed (correct citation). Literally copying of text must be indicated as such by using quotation marks and giving proper reference.

The violation of the Ethical Statement rules may result in severe consequences.

I agree with the above statements and declare that this submission follows the policies of Remote Sensing Applications: Society and Environment as outlined in the Guide for Authors and in the Ethical Statement.

Funding

This work was supported by the Miguel Hernández University of Elche Vicerectorate for Research [grant number VIPROY22/30].

Declaration of competing interest

The author declares that he has no known competing financial interests or personal relationships that could have appeared to influence the work reported in this paper.

Data availability

Data will be made available on request.

References

AEMET, 2022. 2022: an early, intense and extensive heat wave. Spanish Meteorological Agency (AEMET) official blog [WWW Document]. https://aemetblog.es/2022/06/22/junio-de-2020-una-ola-de-calor-temprana-intensa-y-extensa/ (accessed 7.10.24).

AEMET-IMP, 2011. Iberian climate atlas. Air temperature and precipitation (1971-2000). Agencia Estatal de Meteorología, Ministerio de Medio Ambiente y Medio Rural y Marino - Instituto de Meteorologia de Portugal. Madrid, Spain.

Albaladejo-García, J.A., Alcon, F., Martínez-Paz, J.M., 2020. The irrigation cooling effect as a climate regulation service of agroecosystems. Water 12. https://doi.org/10.3390/W12061553, 1553 12, 1553.

Altieri, M.A., 2002. Agroecology: the science of natural resource management for poor farmers in marginal environments. Agric. Ecosyst. Environ. 93, 1–24. https://doi.org/10.1016/S0167-8809(02)00085-3.

Aram, F., Higueras García, E., Solgi, E., Mansournia, S., 2019. Urban green space cooling effect in cities. Heliyon 5, e01339. https://doi.org/10.1016/j.heliyon.2019.

Ballester, J., Quijal-Zamorano, M., Méndez Turrubiates, R.F., Pegenaute, F., Herrmann, F.R., Robine, J.M., Basagaña, X., Tonne, C., Antó, J.M., Achebak, H., 2023. Heat-related mortality in Europe during the summer of 2022. Nat. Med. 23. https://doi.org/10.1038/s41591-023-02419-z.

Bonfils, C., Lobell, D., 2007. Empirical evidence for a recent slowdown in irrigation-induced cooling. Proc. Natl. Acad. Sci. U. S. A. 104, 13582–13587. https://doi.org/10.1073/PNAS.0700144104/SUPPL FILE/00144FIGS.PDF.

Boudjellal, L., Bourbia, F., 2018. An evaluation of the cooling effect efficiency of the oasis structure in a Saharan town through remotely sensed data. Int. J. Environ. Stud. 75, 309–320. https://doi.org/10.1080/00207233.2017.1361610.

Castelli, G., Castelli, F., Bresci, E., 2019. Mesoclimate regulation induced by landscape restoration and water harvesting in agroecosystems of the horn of Africa. Agric. Ecosyst. Environ. 275, 54–64. https://doi.org/10.1016/J.AGEE.2019.02.002.

Chao, C.C.T., Krueger, R.R., 2007. The date palm (Phoenix dactylifera L.): overview of biology, uses, and cultivation. Hortscience 42, 1077–1082. https://doi.org/10.21273/hortsci.42.5.1077.

Copernicus, 2022. OBSERVER: A Wrap-Up of Europe's Summer 2022 Heatwave. Copernicus.

Cuerdo-Vilches, T., Díaz, J., López-Bueno, J.A., Luna, M.Y., Navas, M.A., Mirón, I.J., Linares, C., 2023. Impact of urban heat islands on morbidity and mortality in heat waves: observational time series analysis of Spain's five cities. Sci. Total Environ. 890. https://doi.org/10.1016/j.scitotenv.2023.164412.

de Haan, W.P., Quintana, R., Vilas, C., Cózar, A., Canals, M., Uviedo, O., Sanchez-Vidal, A., 2023. The dark side of artificial greening: plastic turfs as widespread pollutants of aquatic environments. Environ. Pollut. 334. https://doi.org/10.1016/j.envpol.2023.122094.

Dunn, O.J., 1964. Multiple comparisons using rank sums. Technometrics 6, 241-252. https://doi.org/10.1080/00401706.1964.10490181.

Earth Resources Observation and Science (EROS) Center, 2020. Landsat 8-9 operational land imager/thermal infrared sensor level-2, collection 2. U.S. Geological Survey. https://doi.org/10.5066/P9OGBGM6.

EEA, 2020. Healthy Environment, Healthy Lives: How the Environment Influences Health and Well-Being in Europe. European Environment Agency (EEA), Luxembourg, Luxembourg.

Eon, R., Wenny, B.N., Poole, E., Eftekharzadeh Kay, S., Montanaro, M., Gerace, A., Thome, K.J., 2024. Landsat 9 thermal infrared sensor-2 (TIRS-2) pre- and post-launch spatial response performance. Remote Sens. 16. https://doi.org/10.3390/RS16061065, 1065 16. 1065.

Friedman, M., 1937. The use of ranks to avoid the assumption of normality implicit in the analysis of variance. J. Am. Stat. Assoc. 32, 675–701. https://doi.org/10.1080/01621459.1937.10503522.

Gobierno de España, 2023. Áreas urbanas en España 2023. Ministerio de Vivienda y Agenda Urbana. Gobierno de España, Madrid, España.

Grimm, N.B., Faeth, S.H., Golubiewski, N.E., Redman, C.L., Wu, J., Bai, X., Briggs, J.M., 2008. Global change and the ecology of cities. Science 319, 756–760. https://doi.org/10.1126/science.1150195, 1979.

Guo, J., Niu, H., Xiao, D., Sun, X., Fan, L., 2021. Urban Green-space Water-consumption characteristics and its driving factors in China. Ecol. Indic. 130, 108076. https://doi.org/10.1016/J.ECOLIND.2021.108076.

Hernández, E.I., Ferrer, M.T., Navarro-Pedreño, J., Melendez-Pastor, I., Gómez, I., 2014. Ancient sustainability use of "the Palmeral of Elche" and the current unsustainability: reasons for a sustainable future. In: Sustainability behind Sustainability, pp. 73–85.

He, X., Zhou, Y., 2024. Urban spatial growth and driving mechanisms under different urban morphologies: an empirical analysis of 287 Chinese cities. Landsc. Urban Plann. 248, 105096. https://doi.org/10.1016/j.landurbplan.2024.105096.

Hsu, A., Sheriff, G., Chakraborty, T., Manya, D., 2021. Disproportionate exposure to urban heat island intensity across major US cities. Nat. Commun. 12, 1–11. https://doi.org/10.1038/s41467-021-22799-5.

Huang, G., Cadenasso, M.L., 2016. People, landscape, and urban heat island: dynamics among neighborhood social conditions, land cover and surface temperatures. Landsc. Ecol. 31, 2507–2515. https://doi.org/10.1007/s10980-016-0437-z.

INE, 2024. INEbase. Spanish national Institute of statistics (INE) [WWW document]. www.ine.es, 2.15.24.

Jayasinghe, S., Jayasooriya, V., Dassanayake, S., 2024. Effects of street tree configuration on urban heat island mitigation. In: Pigliautile, I., Piselli, C., Karunathilake, H.P., Fabiani, C. (Eds.), Urban Resilience, Livability, and Climate Adaptation. Health, Environmental Dynamics, and Societal Well-Being. Springer Nature, Switzerland, Cham, Switzerland, pp. 3–13. https://doi.org/10.1007/978-3-031-54911-3_1.

Jenerette, G.D., Harlan, S.L., Stefanov, W.L., Martin, C.A., 2011. Ecosystem services and urban heat riskscape moderation: water, green spaces, and social inequality in Phoenix, USA. Ecol. Appl. 21, 2637–2651. https://doi.org/10.1890/10-1493.1.

Kalnay, E., Cai, M., 2003. Impact of urbanization and land-use change on climate. Nature 423, 528-531. https://doi.org/10.1038/nature01675.

Kim, J., Khouakhi, A., Corstanje, R., Johnston, A.S.A., 2024. Greater local cooling effects of trees across globally distributed urban green spaces. Sci. Total Environ. 911, 168494. https://doi.org/10.1016/j.scitotenv.2023.168494.

Krueger, R.R., 2021. Date palm (phoenix dactylifera L.) biology and utilization. In: Jameel, M., Al-Khayri, J.M., Jain, S.M., Johnson, D.V. (Eds.), The Date Palm Genome, Vol. 1. Phylogeny, Biodiversity and Mapping. Springer International Publishing, Cham, Switzerland, pp. 3–28. https://doi.org/10.1007/978-3-030-73746-7.1

Kruskal, W.H., Wallis, W.A., 1952. Use of ranks in one-criterion variance analysis. J. Am. Stat. Assoc. 47, 583-621.

Lalouani, S., Alkama, D., 2012. Palm trees reuses as sustainable element in the Sahara. The case of Ziban, as self-sustainable urban units. Energy Proc. 18, 1076–1085. https://doi.org/10.1016/j.egypro.2012.05.122.

Larrosa Rocamora, J.A., 2003. El Palmeral de Elche. Evolución reciente y función turística después de su declaración como Patrimonio de la Humanidad. Ciudad Territ. - Estud. Territ. 35, 127–154.

Lilliefors, H.W., 1967. On the Kolmogorov-smirnov test for normality with mean and variance unknown. J. Am. Stat. Assoc. 62, 399-402.

Li, S., Zhu, Y., Wan, H., Xiao, Q., Teng, M., Xu, W., Qiu, X., Wu, X., Wu, C., 2024. Effectiveness of potential strategies to mitigate surface urban heat island: a comprehensive investigation using high-resolution thermal observations from an unmanned aerial vehicle. Sustain. Cities Soc. 113, 105716. https://doi.org/10.1016/j.scs.2024.105716.

Liu, X., Hu, G., Chen, Y., Li, X., Xu, X., Li, S., Pei, F., Wang, S., 2018. High-resolution multi-temporal mapping of global urban land using Landsat images based on the Google Earth Engine Platform. Remote Sens. Environ. 209, 227–239. https://doi.org/10.1016/j.rse.2018.02.055.

Li, Y., Schubert, S., Kropp, J.P., Rybski, D., 2020. On the influence of density and morphology on the Urban Heat Island intensity. Nat. Commun. 11, 1–9. https://doi.org/10.1038/s41467-020-16461-9.

MAPA, 2024. Agroclimatic information system for irrigation (SIAR). Ministry of Agriculture, Fisheries and Food (MAPA). Government of Spain [WWW Document]. https://servicio.mapa.gob.es/websiar/, 2.26.24.

Martínez-Fernández, J., Esteve-Selma, M.A., Baños-González, I., Carreño, F., Moreno, A., 2013. Sustainability of Mediterranean irrigated agro-landscapes. Ecol. Model. 248, 11–19. https://doi.org/10.1016/j.ecolmodel.2012.09.018.

Mashhoodi, B., Unceta, P.M., 2024. Urban form and surface temperature inequality in 683 European cities. Sustain. Cities Soc. 113, 105690. https://doi.org/10.1016/j.scs.2024.105690.

Matallah, M.E., Ahriz, A., Zitouni, D.C., Arrar, H.F., Ratmia, M., Attia, S., 2023. A methodological approach to evaluate the passive cooling effect of Oasis palm groves. Sustain. Cities Soc. 99, 104887. https://doi.org/10.1016/j.scs.2023.104887.

Mazzone, A., De Cian, E., Falchetta, G., Jani, A., Mistry, M., Khosla, R., 2023. Understanding systemic cooling poverty. Nat. Sustain. 6, 1533–1541. https://doi.org/10.1038/s41893-023-01221-6.

Melendez-Pastor, I., Navarro-Pedreño, J., Wittenberg, H., 2015. Watermills in the historic irrigation system "Palmeral de Elche". Spain: An example of early hydropower exploitation. Water Sci Technol Water Supply 15, 1140–1151. https://doi.org/10.2166/ws.2015.067.

Namazi, Y., Charlesworth, S., Montazami, A., Taleghani, M., 2024. The impact of local microclimates and Urban Greening Factor on schools' thermal conditions during summer: a study in Coventry, UK. Build. Environ. 262, 111793. https://doi.org/10.1016/j.buildenv.2024.111793.

Navarro-Leblond, M., Meléndez-Pastor, I., Navarro-Pedreño, J., Gómez-Lucas, I., 2021. Soil sealing and hydrological changes during the development of the university campus of Elche (Spain). Int. J. Environ. Res. Publ. Health 18, 9511.

Newsome, M., 2023. Islands of illness. Sci. Am. 621, s48-s49. https://doi.org/10.1038/scientificamerican1023-s26.

Oke, T.R., 1976. The distinction between canopy and boundary-layer urban heat Islands. Atmosphere 14, 268–277. https://doi.org/10.1080/00046973.1976.9648422.

 $Oke, T.R., 1973. \ City \ size \ and \ the \ urban \ heat \ island. \ Atmos. \ Environ. \ (7), 769-779. \ https://doi.org/10.1016/0004-6981(73)90140-6, 1967. \ https://doi.org/10.1016/0004-6981(73)90140-6, 19$

Pablo Martínez, L., Pineda Pérez, E., 2003. El Palmeral de Elche. Un paisaje cultural heredado de Al-Andalus. Ajuntament d'Elx, Elche. España.

Paudel, S., States, S.L., 2023. Urban green spaces and sustainability: exploring the ecosystem services and disservices of grassy lawns versus floral meadows. Urban For. Urban Green. 84, 127932. https://doi.org/10.1016/j.ufug.2023.127932.

Pearlmutter, D., Krüger, E.L., Berliner, P., 2009. The role of evaporation in the energy balance of an open-air scaled urban surface. Int. J. Climatol. 29, 911–920. https://doi.org/10.1002/JOC.1752.

- Phelan, P.E., Kaloush, K., Miner, M., Golden, J., Phelan, B., Silva, H., Taylor, R.A., 2015. Urban heat island: mechanisms, implications, and possible remedies. Annu. Rev. Environ. Resour. 40, 285–307. https://doi.org/10.1146/annurev-environ-102014-021155.
- Probst, N., Bach, P.M., Cook, L.M., Maurer, M., Leitão, J.P., 2022. Blue Green Systems for urban heat mitigation: mechanisms, effectiveness and research directions. Blue-Green Systems 4, 348–376. https://doi.org/10.2166/BGS.2022.028.
- R Core Team, 2023. R: A Language and Environment for Statistical Computing. R Foundation for Statistical Computing, Vienna, Austria [WWW Document]. http://www.r-project.org, 1.15.23.
- Reuter, D.C., Richardson, C.M., Pellerano, F.A., Irons, J.R., Allen, R.G., Anderson, M., Jhabvala, M.D., Lunsford, A.W., Montanaro, M., Smith, R.L., Tesfaye, Z., Thome, K.J., 2015. The thermal infrared sensor (TIRS) on landsat 8: Design overview and pre-launch characterization. Remote Sens. 7, 1135–1153. https://doi.org/10.3390/rs70101135.
- Rodríguez-Rojas, M.I., Grindlay Moreno, A.L., 2022. A discussion on the application of terminology for urban soil sealing mitigation practices. Int. J. Environ. Res. Publ. Health 19, 8713.
- Ruiz-Navarro Ribalaygua, M., 2014. Censo del Palmeral Histórico de Elche 2013. In: El Palmeral Ilicitano: Presente Y Futuro. Cátedra Palmeral d'Elx, Elche, España, p. 20.
- Saaroni, H., Amorim, J.H., Hiemstra, J.A., Pearlmutter, D., 2018. Urban Green Infrastructure as a tool for urban heat mitigation: survey of research methodologies and findings across different climatic regions. Urban Clim. 24, 94–110. https://doi.org/10.1016/J.UCLIM.2018.02.001.
- Sharma, A.K., Gardner, T., Begbie, D. (Eds.), 2019. Approaches to Water Sensitive Urban Design. Potential, Design, Ecological Health, Urban Greening, Policies, and Community Perceptions. Elsevier, Amsterdam, Netherlands. https://doi.org/10.1016/c2016-0-03594-5.
- Stuhlmacher, M., Georgescu, M., Turner, B.L., Hu, Y., Goldblatt, R., Gupta, S., Frazier, A.E., Kim, Y., Balling, R.C., Clinton, N., 2022. Are global cities homogenizing? An assessment of urban form and heat island implications. Cities 126. https://doi.org/10.1016/j.cities.2022.103705.
- Sun, Y., Jiao, L., Guo, Y., Xu, Z., 2024. Recognizing urban shrinkage and growth patterns from a global perspective. Appl. Geogr. 166, 103247. https://doi.org/10.1016/j.apgeog.2024.103247.
- Tengberg, M., 2012. Beginnings and early history of date palm garden cultivation in the Middle East. J. Arid Environ. 86, 139–147. https://doi.org/10.1016/j.
- UN DESA, 2019. World population prospects 2019 [WWW document]. https://population.un.org/wpp/, 4.25.22.
- UNESCO, 2024. Palmeral of Elche [WWW document]. UNESCO World heritage convention. World heritage list-dossier 930. https://whc.unesco.org/en/list/930, 6.16.24.
- USGS, 2024. Landsat 8-9 Collection 2 (C2) Level 2 Science Product (L2SP) Guide. Sioux Falls (SD), USA. Version 6. May 2024.
- van Huijgevoort, M.H.J., Cirkel, D.G., Voeten, J.G.W.F., 2024. Climate adaptive solution for artificial turf in cities: integrated rainwater storage and evaporative cooling. Frontiers in Sustainable Cities 6, 1–11. https://doi.org/10.3389/frsc.2024.1399858.
- Xu, L., Shi, Z., Wang, Y., Chu, X., Yu, P., Xiong, W., Zuo, H., Zhang, S., 2017. Agricultural irrigation-induced climatic effects: a case study in the middle and southern Loess Plateau area, China. Int. J. Climatol. 37, 2620–2632. https://doi.org/10.1002/JOC.4869.
- Yang, M., Ren, C., Wang, H., Wang, J., Feng, Z., Kumar, P., Haghighat, F., Cao, S.-J., 2024. Mitigating urban heat island through neighboring rural land cover. Nature Cities 1. https://doi.org/10.1038/s44284-024-00091-z.
- Zhou, X., Chen, H., 2018. Impact of urbanization-related land use land cover changes and urban morphology changes on the urban heat island phenomenon. Sci. Total Environ. 635, 1467–1476. https://doi.org/10.1016/J.SCITOTENV.2018.04.091.